Journal of Magnetic Resonance **157,** 171–177 (2002)
doi:10.1006/jmre.2002.2590

Dipole–Dipole Coupling Constant for a Directly Bonded CH Pair—A Carbon-13 Relaxation Study

Jozef Kowalewski,* Maria Effemey,* and Jukka Jokisaari†

*Division of Physical Chemistry, Arrhenius Laboratory, Stockholm University, S-106 91 Stockholm, Sweden; and †Department of Physical Sciences, P.O.Box 3000, FIN-90014 University of Oulu, Finland

Received October 1, 2001; revised May 29, 2002; published online August 28, 2002

Multiple-field (4.7, 9.4, 14.1 T) carbon-13 relaxation data are reported for hexamethylenetetramine (HMTA) in the cryosolvent D_2O/DMSO at 243 K. Under these conditions, the reorientational motion of HMTA is outside of the extreme narrowing range and the relaxation data can be subjected to a quantitative interpretation. Because of the high symmetry of the HMTA molecule, the reorientation must be isotropic. Treating the reorientation as a small-step rotational diffusion of a rigid body, we obtain a rotational correlation time of 1.0 ns and a carbon–proton dipole–dipole coupling constant corresponding to an effective internuclear distance of 114. 2 pm. The harmonic vibrational correction to the dipole–dipole coupling constant, based on a known force field, yields an NMR estimate of the r^{α} distance of 110.8 ± 0.3 pm.

1. INTRODUCTION

Carbon-13 relaxation studies are an important source of information on reorientational molecular dynamics in liquid solutions (*1–3*). For protein work in solution, nitrogen-15 relaxation measurements play a similar role (*3–5*). The relaxation behavior of nitrogen-15 is more complicated, however, and we concentrate in this paper on the carbon-13 case. Proton-carrying carbon-13 nuclei usually relax predominantly by the dipole–dipole interaction with directly bonded protons. One commonly distinguishes between two situations: the extreme narrowing regime, when the molecular motions are fast on the time scale of carbon and proton Larmor frequencies, and the nonextreme narrowing range, when the molecular reorientation is slower. The former range applies to small molecules in low-viscosity solutions and allows very simple interpretation of the data. Working outside of the extreme narrowing, where the nuclear spin relaxation becomes dependent on the magnetic field, requires more measurement and more complicated analysis, but may yield more interesting quantitative results. In this paper, we report a study of a hexamethylenetetramine (HMTA, Fig. 1) solution in a cryosolvent (D_2O/dimethyl sulfoxide (DMSO) in a 2 : 1 molar ratio), which is highly viscous at low temperatures. The high viscosity slows down molecular reorientation so as to bring the motion of HMTA out of extreme narrowing. In this way, we take simultaneous advantage of the fact that we deal with a small, rigid, and highly symmetric molecule and of the possibilities offered by the field dependence of the relaxation data. HMTA has interested NMR spectroscopists for many years, and its dynamic properties have been studied by NMR in both solid state (*6–9*), liquid crystalline mesophase (*10*), and liquid solution (*11, 12*).

If the protons in a molecule are subjected to broadband decoupling, and the cross-correlations between different interactions can be neglected, then the carbon-13 spin–lattice relaxation is a simple exponential process, characterized by a single time constant, T_1, called the spin–lattice relaxation time, or longitudinal relaxation time. Besides the T_1, two additional relaxation parameters are commonly measured and used: the nuclear Overhauser enhancement (NOE) and the spin–spin (or transverse) relaxation time, denoted T_2. Under extreme narrowing conditions, the NOE measurements allow separation of the dipolar and other relaxation mechanisms. Neglecting the contributions from distant (not directly bonded) protons in the extreme narrowing range, the dipolar contribution to the spin–lattice relaxation rate $1/T_{1DD}$ is given by a very simple relation:

$$\frac{1}{T_{1DD}} = n_{\mathrm{H}} D_{\mathrm{CH}}^2 \tau_c^{eff}. \qquad [1]$$

n_{H} is the number of directly bonded protons, D_{CH} is the dipole coupling constant (DCC), and τ_c^{eff} is the effective correlation time. The dynamic information resides in the effective correlation time. Outside of the extreme narrowing regime, the effective correlation time is replaced by a linear combination of spectral density functions, but $1/T_{1DD}$ remains proportional to the square of the dipole coupling constant.

A knowledge of the dipole–coupling constant is thus essential for obtaining dynamic information from carbon-13 relaxation. The DCC (in rad · s^{-1}) is commonly given by a simple relation (*1, 2*),

$$D_{\mathrm{CH}} = -\frac{\mu_0 \gamma_{\mathrm{C}} \gamma_{\mathrm{H}} \hbar}{4\pi} r_{\mathrm{CH}}^{-3}, \qquad [2]$$

where r_{CH} is the carbon–proton distance, and other symbols have their usual meaning. The carbon–hydrogen distance in directly

1090-7807/02 $35.00

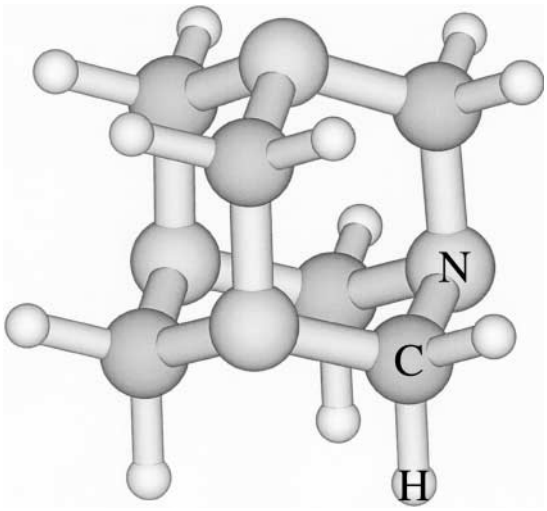

FIG. 1. The structure of HMTA.

bonded $^{13}C^{1}H$ spin systems is approximately known. The *exact* values of r_{CH} that should be used to get a DCC appropriate for the interpretation of relaxation data are not obvious, and values in the 107–114 pm range have been applied. In extreme narrowing, the choice of a particular value within this range has no important consequences. Missetting r_{CH} by a few percent results in a τ_c^{eff} that is perhaps 10–15% off, but this accuracy in the effective correlation time is usually sufficient for qualitative discussions. In many applications, relative values of τ_c^{eff} at different sites in a molecule or in a series of related systems are of interest. These relative values can be obtained more accurately if the r_{CH} values can be assumed to be the same for different CH bonds. For larger molecules, where the motion is outside of the extreme narrowing range, it was recognized early on that a CH distance of about 110 pm (based on neutron diffraction data (*13*)) does not lead to a consistent picture in terms of rigid-body rotation (*14–16*).

The role of vibrational corrections for the DCC in the context of ^{13}C dipolar relaxation has been discussed during the seventies and eighties (*17–20*), while similar work for solutes in liquid crystalline systems was presented even earlier (*21, 22*) and for solids somewhat later (*23–25*). In the carbon relaxation work from the mid-eighties and to the present date, the nonrigidity of molecules has often been treated within the framework of the Lipari-Szabo (model-free) approach (*26*). In this approach, the exact value of the DCC is again of minor importance: a possible missetting leads only to changes in the generalized order parameter, a quantity whose relative values within a molecule or in a series of related molecules are usually more interesting than the absolute ones. For example, in a series of papers on oligosaccharides from one of our laboratories (*27–33*), we have consistently used the $r_{CH} = 109.8$ pm. The issue of the accurate carbon–proton DCCs has attracted renewed interest in the past few years. Ottiger and Bax (*34*) determined effective $C^{\alpha}H^{\alpha}$ bond length in a protein, using a dilute liquid crystalline phase as a solvent. Kowalewski and co-workers (*35*), Gryff-Keller and Molchanov (*36*), and Hardy and co-workers (*37, 38*) discussed systems where more than one carbon-13 relaxation mechanism needed to be considered and where one of the goals was to determine the interaction strength for the second mechanism. Case reported an analysis of vibrational corrections based on *ab initio* calculations (*39*).

In this paper, we try to answer the question of the magnitude of the carbon–proton DCC and the CH distance by a relaxation approach. We have worked with HMTA as a model system because the overall motion of this molecule must be isotropic for reasons of symmetry. Moreover, it is safe to assume that there are no large-amplitude internal motions and that the harmonic force field for small-amplitude vibrations is known. We studied HMTA in the cryosolvent that we have often used in our oligosaccharide work (*27–32*). Using this solvent and working at a low temperature, to take the system out of extreme narrowing, we derive the DCC and the rotational correlation time from variable-field measurements of carbon-13 T_1, T_2, and NOE. The methods are presented in section 2, the experimental details are given in section 3, the results are discussed in section 4, and the conclusions are drawn in section 5.

2. METHODS

2.1. NMR Relaxation

The dipole–dipole relaxation rates, T_{1DD}^{-1}, T_{2DD}^{-1}, and the NOE are expressed in terms of the DCC and spectral densities as follows (*33*):

$$T_{1DD}^{-1} = \frac{n_H}{4} D_{CH}^2 [J(\omega_H - \omega_C) + 3J(\omega_C) + 6J(\omega_H + \omega_C)] \quad [3]$$

$$T_{2DD}^{-1} = \frac{n_H}{8} D_{CH}^2 [4J(0) + J(\omega_H - \omega_C) + 3J(\omega_C) + 6J(\omega_H) + 6J(\omega_H + \omega_C)] \quad [4]$$

$$\eta = \left(\frac{\gamma_H}{\gamma_C}\right) \frac{6J(\omega_H + \omega_C) - J(\omega_H - \omega_C)}{J(\omega_H - \omega_C) + 3J(\omega_C) + 6J(\omega_H + \omega_C)}. \quad [5]$$

The form of the above expressions [3]–[5] assumes that cross-correlations between different interactions can be neglected. This is not an obvious assumption for an AX_2 spin system with magnetic equivalence, even if the protons (X spins) are subject to double–resonance irradiation. Instead, the spin–lattice relaxation becomes in such a case biexponential, and the expression for NOE attains a more complicated form (*40*). However, as discussed by Werbelow and Grant (*41*), the initial rate of carbon recovery after an inversion is still given by Eq. [1] or [3], while the NOE regains the simplicity of Eq. [5] in the case of isotropic motions.

The form of the spectral density functions $J(\omega)$ depends on the motional model chosen. For the commonly used Lipari-Szabo

(model-free) approach, the spectral density is (*26*)

$$J(\omega)=\frac{2}{5}\left(\frac{S^2\tau_{\mathrm{M}}}{1+\omega^2\tau_{\mathrm{M}}^2}+\frac{(1-S^2)\tau}{1+\omega^2\tau^2}\right), \qquad [6]$$

where $\tau^{-1}=\tau_{\mathrm{M}}^{-1}+\tau_e^{-1}$. τ_{M} is the rotational correlation time for rank 2 spherical harmonics (*1–3*) (the correlation time for the global motion, common to the whole molecule), τ_e is the correlation time for the fast local motion (specific for every individual axis in the molecule), and S is a generalized order parameter for an axis in the molecule. If S^2 is large (the molecule does not have extensive internal mobility), the second term can be neglected and the order parameter squared can be incorporated in the effective DCC (*42, 43*). Henry and Szabo (*20*) demonstrated that the effect of vibrations can rigorously be incorporated into the effective dipole–dipole coupling constant, provided that the vibrationally averaged interaction tensor is axially symmetric. When these conditions apply and the effective DCC is set in Eqs. [3] and [4], the spectral densities take the very simple form corresponding to isotropic rotational diffusion of a rigid body:

$$J(\omega)=\frac{2}{5}\frac{\tau_{\mathrm{M}}}{1+\omega^2\tau_{\mathrm{M}}^2}. \qquad [7]$$

We argue that this simple motional model, including the effects of vibrations into the DCC and expressing the dynamics in terms of Eq. [7], is adequate for HMTA in a viscous solvent. Using the ideas of Case (*39*), this is equivalent to the Lipari-Szabo approach at the rigid limit ($S^2=1$), excluding the thermally activated motions, with the reference state including the zero-point vibrational motions. We note that the T_d symmetry of the molecule guarantees isotropic motion, and the relatively slow reorientation in the viscous solutions makes the small-step diffusion model adequate (*vide infra*). The effective, vibrationally averaged DCC is analogous to the interaction-strength constant describing the dipolar interaction in solid state (*20*). The crystallographic data (*44–46*), the *ab initio* calculations (*46*), and the vibrational spectra of HMTA in solid and in solution (*47–49*) are all consistent with this picture. The lowest vibrational frequency in HMTA corresponds to a wave number of about 450 cm^{-1} (*49*). At the temperature of the NMR experiments, the Boltzmann factor for the lowest vibrationally excited state is about 7%.

2.2. *Vibrational Averaging*

In a molecule which is allowed to have internal vibrations, the r_{CH}^{-3} factor in the expression for the DCC (Eq. [2]) should be replaced by an average over vibrational motions. Considering only internal molecular vibrations, and following Sykora *et al.* (*22*), the experimental dipolar couplings can be represented in the form,

$$D_{\mathrm{CH}}=D_{\mathrm{CH}}^{eq}+d_{\mathrm{CH}}^{h}+d_{\mathrm{CH}}^{ah}, \qquad [8]$$

where D_{CH}^{eq} corresponds to the equilibrium (r_e) structure. The symbols d_{CH}^{h} and d_{CH}^{ah} are harmonic and anharmonic correction terms, respectively. The anharmonic term is often neglected; the structure corrected for the effect of harmonic vibrations is referred to as the r_α structure. The corresponding DCC is

$$D_{\mathrm{CH}}^{\alpha}=D_{\mathrm{CH}}-d_{\mathrm{CH}}^{h} \qquad [9]$$

Detailed information on how the correction terms in Eq. [8] are related to the intramolecular force field and on the normal coordinates can be found in the paper by Sýkora *et al.* (*22*).

3. EXPERIMENTAL

The HMTA was obtained from Aldrich (99+%, Gold label) and was used without further purification. The HMTA sample was dissolved in a 7 : 3 molar ratio mixture of D_2O and DMSO to yield a 240 mM solution. The sample was degassed by several freeze–pump–thaw cycles before being sealed under vacuum in a 5-mm NMR tube.

The carbon-13 NMR experiments were performed at 4.7, 9.4, and 14.1 T. The experiments at 4.7 T were carried out using a Chemagnetics Infinity spectrometer equipped for high-resolution work with a Bruker 5 mm inverse detection probehead, while Varian Inova spectrometers were used at the higher fields. A Varian switchable 5-mm probehead was used at 9.4 T and a Varian 5 mm broadband probehead was used on the 14.1 T spectrometer. Standard variable-temperature controllers from Bruker (at 4.7 T) and Varian were used. Before every measurement, the temperature was carefully checked with a methanol chemical-shift thermometer (*50*). Deuterium lock for field/frequency stabilization was used in all experiments.

The carbon-13 spin–lattice relaxation times (T_1) were measured by the fast inversion–recovery (FIR) method (*51*) with 12–15 different delays. The nuclear Overhauser enhancements were determined by the dynamic NOE (DNOE) technique (*52*), with one long (about 5 T_1) and one short (about 1 ms) delay. The NOE factor, $1+\eta$, is expressed as the intensity ratio of the enhanced signal (long delay in the DNOE experiment) to the unenhanced signal (short delay). The spin–spin relaxation time (T_2) was measured at 9.4 T only, using a modification of the Carr-Purcell-Meiboom-Gill experiments, designed to suppress the cross-correlation effects (*53, 54*). The carbon-13 90° pulse duration was about 15 μs at 4.7 T and 5–7 μs at higher fields. The spectral width was typically 50–100 ppm, the number of data points was about 16 k and the number of transients 128 to 1024. A recycle delay of about 2 times the longest T_1 was used in the FIR experiments, whereas it was about $10T_1$ in the NOE experiments. The broadband proton decoupling was carried out using the Waltz-16 scheme. The typical decoupler 90° pulse duration was about 100–150 μs. A line broadening of 1.5–4 Hz was applied before evaluating line intensities. A three-parameter exponential fitting routine provided by the instrument manufacturers was used to evaluate the spin–lattice and

spin–spin relaxation times. The accuracy of the T_1 data is estimated to be better than 5% (*vide infra*); the accuracy of the NOE factor is estimated to be better than 0.1 units, and the accuracy of the T_2 measurements is better than 10%. All the experiments have been repeated at least twice and average values are reported.

The analysis of the variable-field relaxation data was carried out with the program GENLSS (*55*) running on an IBM RISC 6000 workstation. The vibrational corrections to D_{CH} were performed, as described in the previous section, applying the program VIBR (*22*) running on a PC. The D_{CH} dipolar coupling of HMTA was corrected for harmonic vibrations utilising the force field of Bertie and Solinas (*49*). As the VIBR program (*22*) provides force constants in units of mdyn/Å, the bend and stretch–bend interaction force constants given in the internal displacement coordinate system in Ref. (*49*) had to be scaled properly with bond lengths. The 60 vibrational frequencies of HMTA were reproducible within the same error limits as those of Ref. (*49*).

4. RESULTS AND DISCUSSION

4.1. NMR Relaxation

In the first step of the ^{13}C NMR relaxation study, we measured the ^{13}C T_1 at 9.4 T at different temperatures. The results are summarized in Fig. 2. The goal of this part of the investigation was to select the temperature at which the variable-field study would be carried out. Based on the data in Fig. 2, we chose 243 K as a convenient working temperature at which the carbon relaxation is close to the minimum, i.e., clearly out of the extreme narrowing regime (*2*).

Having established the working temperature, we performed ^{13}C T_1 and NOE experiments at 243 K at three magnetic fields as well as T_2 measurements at 9.4 T. As noted above, the response of the CH_2 carbon-13 magnetization to the inversion–recovery

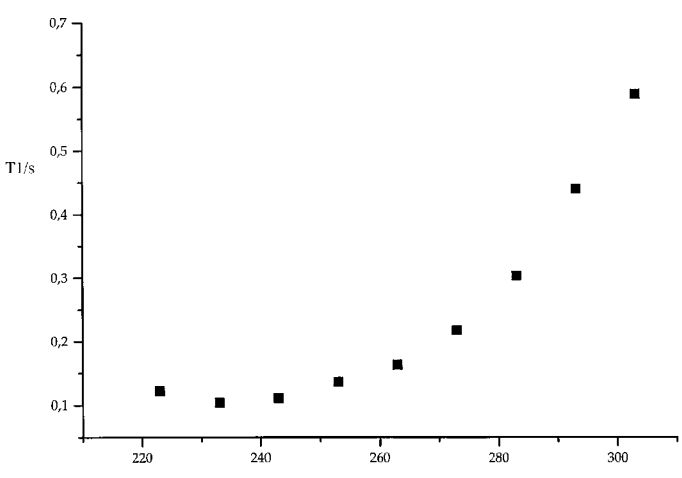

FIG. 2. The temperature dependence of the ^{13}C spin–lattice relaxation rate for HMTA in the D_2O/DMSO cryosolvent.

TABLE 1
The Measured ^{13}C Relaxation Parameters for HMTA in D_2O/DMSO at 243 K as a Function of the Magnetic Field

Relaxation parameter	4.7 T	9.4 T	14.4 T
T_1^{-1}/s^{-1}	7.95	4.83	3.13
T_2^{-1}/s^{-1}	—	6.49	—
$1+\eta$	1.95	1.43	1.29

experiment is in principle biexponential (*40*). We have not seen any experimental evidence of biexponential recovery; the fits to a single exponential relation were excellent in all cases, with standard deviations on the order of 1–2% or less. To further clarify the meaning of our T_1 values, we have estimated the initial rates for some selected experiments. The rates obtained in this way were within 2–4% from the T_1^{-1} values; the uncertainties in the initial rates were in general significantly larger than in the exponential fits. Thus, we shall work with T_1^{-1} values from the exponential fit, but choose a conservative uncertainty of about 5%. In addition, we discuss below how the assumed validity of the single exponential recovery of longitudinal magnetization can be validated *a posteriori*.

The relaxation parameters are collected in Table 1 and presented graphically in Fig. 3. We assume that the carbon–proton dipolar interaction is the only relaxation mechanism active (*vide infra*) and that the field dependence of the relaxation rates and the NOE is given by Eqs. [3]–[5], [2], and [7]. These contain only two adjustable parameters, r_{CH} and τ_M. We fitted these two parameters to the seven data points and obtained $r_{CH} = 114.2 \pm 0.2$ pm and $\tau_M = 1.03 \pm 0.02$ ns (the error limits are one standard

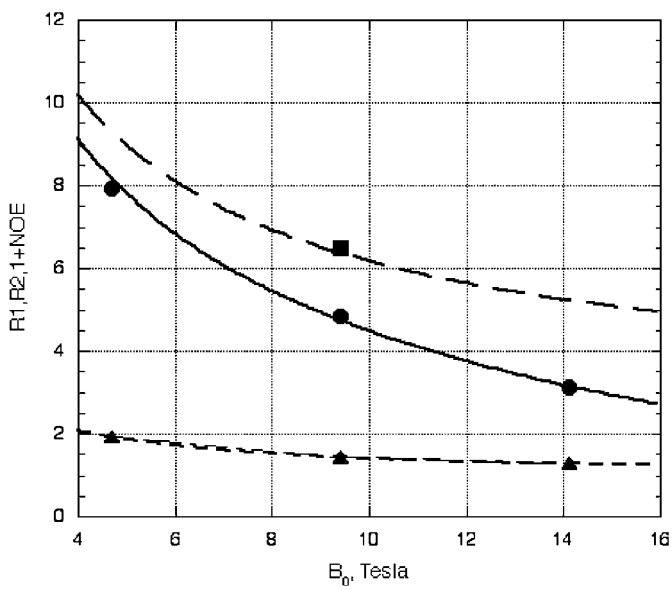

FIG. 3. Theoretical and experimental field dependence of the carbon-13 relaxation parameters for HMTA at 243 K (circles, solid line: R_1; squares, long-dashed line: R_2; triangles, short-dashed line: $1+\eta$).

deviation of the nonlinear fit). Excluding the transverse rate from the fit changed the effective distance by 0.1 pm.

Two brief comments can be made concerning the correlation time. First, we can see that $\omega^2\tau_M^2$ for various nonzero frequencies occurring in Eqs. [3]–[5] range between about 0.1 (when ω is set equal to the carbon Larmor frequency at 4.7 T) and about 25 (when $\omega = \omega_C + \omega_H$ at 14.1 T). Thus, the spectral densities sample a wide range of frequencies outside of the extreme narrowing regime. Second, we can compare τ_M with the free-rotor correlation in the χ test according to Wallach and Huntress (*56*). With a moment of inertia of 6.62×10^{-45} kg m^2 (based on the crystal structure (*43–45*)), the free-rotor correlation time (τ_f) at 243 K is about 0.84 ps, and the ratio, $\chi = \tau_M/\tau_f$ is about 1200. Wallach and Huntress (*56*) state that if $\chi \gg 1$, then the rotational motion is in the small-step diffusion limit, which in indeed is the case for our system.

The question of the effective DCC or the effective carbon–proton bond length is more interesting and more difficult. The effective distance of 114.2 pm obtained from NMR relaxation (corresponding to a DCC of 1.274×10^5 rad s^{-1}) is substantially longer than the neutron-scattering CH distance of 109.7 pm in HMTA, from Kampermann *et al.* (*45*). It is well-known that vibrational averaging leads to effective distances longer than those obtained from neutron scattering (*19*), but we find the difference between 114.2 and 109.7 pm larger than expected. Our effective CH distance is also significantly longer than the results of Ottiger and Bax (*34*) (111.7 ± 0.7 pm for the $C^\alpha H^\alpha$ bond length in a protein) and of Case (*39*) (111.3 pm for the $C^\alpha H^\alpha$ bond length in a peptide).

In order to investigate possible error sources, we have taken the measures described below. First, we investigated the effects of the biexponential longitudinal ^{13}C relaxation, described by the following equation (*40*):

$$-\frac{d}{dt}\begin{pmatrix} y_2(t) \\ y_{3'}(t) \end{pmatrix} = \begin{pmatrix} \Gamma_{11} & \Gamma_{12} \\ \Gamma_{12} & \Gamma_{22} \end{pmatrix}\begin{pmatrix} y_2(t) \\ y_{3'}(t) \end{pmatrix} + \begin{pmatrix} \Gamma_{13} \\ \Gamma_{23} \end{pmatrix}. \quad [10]$$

Using the rotational correlation time and the effective DCC estimated above, as well as an assumed angle between the CH vectors, $\theta_{HCH} = 109.5°$, we have calculated all the elements Γ_{ij} in Eq. [10] using the expressions given by Werbelow and Grant (*40*) at each of our three magnetic fields. Nondipolar effects were neglected (*vide infra*). The biexponential solutions were obtained and the time course of the longitudinal carbon-13 magnetization ($y_2(t)$ in Eq. [10]) after the initial inversion was computed at a selection of time points mimicking our inversion–recovery experiments. These calculated "theoretical data points" were subjected to a single exponential fit, yielding a "theoretical single exponential rate." This rate was compared with the T_{1DD}^{-1} of Eq. [3] (this T_{1DD}^{-1} is identical to Γ_{11} in Eq. [10]). The theoretical single exponential rate was about 1.5–2.1% lower than T_{1DD}^{-1}. We repeated also the same procedure with θ_{HCH} increased or reduced by 3°. The maximum reduction of the theoretical rate was 2.7% at $\theta_{HCH} = 106.5°$ and 1.5% at $\theta_{HCH} = 112.5°$. Based on these results, we conclude that the errors in T_{1DD}^{-1} caused by neglecting the coupling terms Γ_{12} in Eq. [10] (the effect of cross-correlation between the two dipolar CH interactions) are systematic, in the sense that they always underestimate the sum of the spectral densities in Eq. [3], but very small. The DCC based on the corrected T_{1DD}^{-1} would thus be slightly larger and the effective distance slightly shorter. The effect of the 3% underestimation of T_{1DD}^{-1} on the effective distance would be about 0.5%.

As a second measure, we have tried to estimate the effects of other possible relaxation mechanisms. To that end, we measured the NOE for ^{13}C in HMTA at room temperature, where extreme narrowing conditions are expected to prevail. The result was $1 + \eta = 2.9$ (±0.1). Since the corresponding quantity for purely dipolar relaxation in extreme narrowing is 2.99, we may have, at room temperature, up to 6% contribution from other relaxation mechanisms (such as ^{13}C–^{14}N dipolar interactions and chemical shielding anisotropy). We attempted to repeat the fitting of the low-temperature data assuming a 3% contribution of other mechanisms to T_1^{-1} and T_2^{-1} as well as a corresponding reduction in the NOE. This correction led, however, to an even slightly smaller DCC or a longer r_{CH} value. A similar effect would be obtained by including the relaxation effect of the distant protons. The correction for other mechanisms and protons other than directly bonded would thus counteract the cross-correlation corrections. Therefore, in order to solve the mystery of this long effective r_{CH}, we decided to turn to a proper calculation of the vibrational corrections.

4.2. Vibrational Averaging

As the anharmonic force constants are (to the best of our knowledge) not known for HMTA, we restrict vibrational averaging exclusively to a harmonic force field as given in Ref. (*49*). Application of harmonic vibrations leads to the correction term d_{CH}^h (cf. Eqs. [8] and [9]), which amounts to 9.0% to the experimental D_{CH} as determined from the relaxation data. This correction *increases* the experimental coupling, and consequently *decreases* the bond length by 3.0%, resulting in the so-called r^α structure. In the present case the r_{CH} of 114.2 pm reduces to $r_{CH}^\alpha = 110.8 \pm 0.3$ pm, where the error limits include experimental error and a possible 4% error in the harmonic correction (*22*).

5. CONCLUDING REMARKS

Recent neutron diffraction studies of HMTA produced refined structures with CH distances of 107.1 pm (*43*) and of 109.4 to 109.7 pm (*44*). The differences have their source in the different treatment of vibrational motions, both the intramolecular vibrations and the librations/translations of the molecules in the crystal lattice. The study of Kampermann *et al.* (*45*) covered measurements over a broad temperature range. The refinement of the diffraction intensities (*44, 45*) was performed taking at

least some anharmonicity into consideration, and the latter results can be judged as good estimates of the r_e structure. *The ab initio* calculations at the RHF level with the 6-311G** basis set yielded a carbon–proton r_e of 108.4 pm (*45*). Our r_α of 110.8 pm must be considered to be in reasonably good agreement with these studies.

The differences between our results and the protein or peptide data of Ottiger and Bax (*34*) and Case (*39*) may have two origins: first, the treatments of vibrational corrections are not identical. Second, the effective CH distance for an α-carbon in peptides may differ from the CH_2 group in HMTA.

Thus, we conclude that the results of our carbon-13 relaxation study outside of extreme narrowing region can be understood in a quantitative sense. The simple dynamic model of a rigid-body rotational diffusion in small steps is fully adequate if one works in terms of an effective dipole–dipole coupling constant. The effective DCC corresponds to a CH distance that differs considerably from the crystallographic distance. Most of this difference can be accounted for by the effect of averaging of the dipolar coupling constant by harmonic vibrations.

ACKNOWLEDGMENTS

We are grateful to Professor Malcolm Levitt, Professor John Bertie, and Professor Lawrence Werbelow for valuable discussions and to Mr. Zdenek Tosner for his assistance with the analysis of biexponential relaxation. This work has been supported by the Swedish Research Council (J.K.) and the Academy of Finland (J.J.).

REFERENCES

1. J. Kowalewski, Nuclear spin relaxation in diamagnetic fluids. Part 2. Organic systems and solutions of macromolecules and aggregates, *Ann. Rep. NMR Spectr.* **23,** 289–374 (1991).
2. G. C. Levy and D. J. Kerwood, *in* "Encyclopedia of Nuclear Magnetic Resonance" (D. M. Grant and R. K. Harris, Eds.), p. 1147, Wiley, Chichester (1996).
3. V. A. Daragan and K. H. Mayo, Motional model analyses of protein and peptide dynamics using C-13 and N-15 NMR relaxation, *Progr. Nucl. Magn. Reson. Spectr.* **31,** 63–105 (1997).
4. A. G. Palmer, Probing molecular motion by NMR, *Curr. Opin. Struct. Biol.* **7,** 732–737 (1997).
5. D. A. Torchia, *in* "Encyclopedia of Nuclear Magnetic Resonance" (D. M. Grant and R. K. Harris, Eds.), p. 3785, Wiley, Chichester (1996).
6. O. Pschorn and H. W. Spiess, Deuterium lineshape study of tetrahedral jumps in solid hexamethylenetetramine, *J. Magn. Reson.* **39,** 217–228 (1980).
7. E. A. Hill and J. P. Yesinowski, Solid-state ^{14}N NMR techniques for studying slow molecular motions, *J. Chem. Phys.* **107,** 346–354 (1997).
8. Y. S. Kye and G. S. Harbison, N-14 NMR single-crystal study of hexamethylenetetramine, *Magn. Reson. Chem.* **37,** 299–302 (1999).
9. G. W. Smith, Proton magnetic resonance studies on hexamethylenetetramine—Structure, molecular reorientation, and impurity diffusion, *J. Chem. Phys.* **36,** 3081–3093 (1962).
10. A. Amanzi, P. L. Barili, P. Chidichimo, and C. A. Veracini, Proton magnetic resonance spectrum of hexamethylenetetramine (HMTA) in oriented mesophases, *Chem. Phys. Lett.* **44,** 110–113 (1976).
11. B. Parbhoo and O. B. Nagy, Multinuclear approach to establish molecular dynamics in solution by nuclear magnetic relaxation, *J. Phys. Chem.* **89,** 239–241 (1985).
12. D. J. Craik, G. C. Levy, and A. Lombardo, Carbon-13 and nitrogen-15 NMR of polycyclic polyamines. A study of solution nitrogen-hydrogen hydrogen bonding and protonation, *J. Phys. Chem.* **86,** 3893–3900 (1982).
13. G. Jeffrey, *in* "Accurate Molecular Structures, Their Determinations and Importance" (A. Domenicano and I. Hargittai, Eds.), p. 270, Oxford Univ. Press, Oxford (1992).
14. M. Llinas, W. Meier, and K. Wüthrich, A carbon-13 spin lattice relaxation of alumichrome at 25.1 MHz and 90.5 MHz, *Biochim. Biophys. Acta* **492,** 1–11 (1977).
15. K. Dill and A. Allerhand, Small errors in CH bond lengths may cause large errors in rotational correlation times determined from carbon-13 spin-lattice relaxation measurements, *J. Am. Chem. Soc.* **101,** 4376–4378 (1979).
16. M. F. Brown, Unified picture for spin-lattice relaxation of lipid bilayers and biomembranes, *J. Chem. Phys.* **80,** 2832–2836 (1984).
17. N. M. Szeverenyi, R. R. Vold, and R. L. Vold, Mechanisms of nuclear magnetic relaxation in cyanoacetylene, *Chem. Phys.* **18,** 23–30 (1976).
18. R. R. Vold, P. H. Kobrin, and R. L. Vold, Frequency dependent nuclear relaxation of chloroform in isotropic MBBA, *J. Chem. Phys.* **69,** 3430–3431 (1978).
19. O. Söderman, The interaction constants in ^{13}C and ^{2}H NMR relaxation studies, *J. Magn. Reson.* **68,** 296–302 (1986).
20. E. R. Henry and A. Szabo, Influence of vibrational motion on solid state line shapes and NMR relaxation, *J. Chem. Phys.* **82,** 4753–4761 (1985).
21. L. C. Snyder and S. Meiboom, Molecular structure of cyclopropane from its proton NMR in a nematic solvent, *J. Chem. Phys.* **47,** 1480–1487 (1967).
22. S. Sýkora, J. Vogt, H. Bösiger, and P. Diehl, Vibrational corrections in NMR spectra of oriented molecules, *J. Magn. Reson.* **36,** 53–60 (1979).
23. T. Terao, H. Miura, and A. Saika, Dipolar SASS NMR spectroscopy: Separation of heteronuclear dipolar powder patterns in rotating solids, *J. Chem. Phys.* **85,** 3816–3826 (1986).
24. T. Nakai, J. Ashida, and T. Terao, Influence of small-amplitude motions on two-dimensional NMR powder patterns. Anisotropic vibrations in calcium formate, *Mol. Phys.* **67,** 839–847 (1989).
25. Y. Ishii, T. Terao, and S. Hayashi, Theory and simulation of vibrational effects on structural measurements by solid-state NMR, *J. Chem. Phys.* **107,** 2760–2774 (1997).
26. G. Lipari and A. Szabo, Model-free approach to the interpretation of nuclear magnetic resonance relaxation in macromolecules 1. Theory and range of validity, *J. Am. Chem. Soc.* **104,** 4546–4559 (1982).
27. J. Kowalewski and G. Widmalm, Multiple-field carbon-13 NMR relaxation study of cyclodextrins, *J. Phys. Chem.* **98,** 28–34 (1994).
28. L. Mäler, J. Lang, G. Widmalm, and J. Kowalewski,Multiple-field carbon-13 NMR relaxation investigation on melezitose, *Magn. Reson. Chem.* **33,** 541–548 (1995).
29. L. Mäler, G. Widmalm, and J. Kowalewski, Dynamical behavior of carbohydrates as studied by carbon-13 and proton nuclear spin relaxation, *J. Phys. Chem.* **100,** 17103–17110 (1996).
30. L. Mäler, G. Widmalm, and J. Kowalewski, Motional properties of a pentasaccharide containing a 2,6-branched mannose residue as studied by 13C nuclear spin relaxation, *J. Biomol. NMR* **7,** 1–7 (1996).
31. A. Kjellberg, T. Rundlöf, J. Kowalewski, and G. Widmalm, Motional properties of two vicinally disubstituted trisaccharides as studied by multiple-field carbon-13 NMR relaxation, *J. Phys. Chem. B* **102,** 1013–1020 (1998).
32. M. Effemey, J. Lang, and J. Kowalewski, Multiple-field carbon-13 and proton relaxation in sucrose in viscous solution, *Magn. Reson. Chem.* **38,** 1012–1018 (2000).

33. T. Rundlöf, R. M. Venable, R. W. Pastor, J. Kowalewski, and G. Widmalm, Distinguishing anisotropy and flexibility of the pentasaccharide LNF- 1 in solution by carbon-13 NMR relaxation and hydrodynamic modeling, *J. Am. Chem. Soc.* **121,** 11847–11854 (1999).
34. M. Ottiger and A. Bax, Determination of relative N-H^N, N-C′, C^α-C′, and C^α-H^α effective bond lengths in a protein by NMR in a dilute liquid crystalline phase, *J. Am. Chem. Soc.* **120,** 12334–12341 (1998).
35. M. Shultes, R. Eisenhauer, J. J. Dechter, M. Johansson, P. Kumar, and J. Kowalewski, Multiple field carbon-13 NMR relaxation of calix[4]arene in solution, *Magn. Reson. Chem.* **37,** 799–804 (1999).
36. A. Gryff-Keller and S. Molchanov, Carbon-13 and mercury-199 nuclear spin relaxation study on solution dynamics of the bis(phenylethynyl)mercury molecule and shielding anisotropy of its acetylenic carbon and mercury nuclei, *Magn. Reson. Chem.* **38,** 1, 17–22 (2000).
37. E. H. Hardy, R. Witt, A. Dölle, and M. D. Zeidler, A new method for the determination of the dynamic isotope effect and the deuterium quadrupole coupling constant in liquids, *J. Magn. Reson.* **134,** 300–307 (1998).
38. E. H. Hardy, A. Zygar, and M. D. Zeidler, Nuclear magnetic relaxation measurements on liquid acetonitrile and acetonitrile water mixtures, *Z. Phys. Chem.* **214,** 1633–1657 (2000).
39. D. A. Case, Calculations of NMR dipolar coupling strength in model peptides, *J. Biomol. NMR* **15,** 95–102 (1999).
40. L. G. Werbelow and D. M. Grant, Proton-decoupled carbon-13 relaxation in $^{13}CH_2$ and $^{13}CH_3$ spin systems, *J. Chem. Phys.* **63,** 4742–4749 (1975).
41. L. G. Werbelow and D. M. Grant, Intramolecular dipolar relaxation in multispin systems, *Adv. Magn. Reson.* **9,** 189–299 (1977).
42. D. C. McCain and J. L. Markley, Rotational spectral density functions for aqueous sucrose: Experimental determination using ^{13}C NMR, *J. Am. Chem. Soc.* **108,** 4259–4264 (1986).
43. H. Kovacs, S. Bagley, and J. Kowalewski, Motional properties of two disaccharides in solutions as studied by carbon-13 relaxation and NOE outside of the extreme narrowing region, *J. Magn. Reson.* **85,** 530–541 (1989).
44. M. Terpstra, B. M. Craven, and R. F. Stewart, Hexamethylenetetramine at 298 K: New refinements, *Acta Crystallogr.* **A49,** 685–692 (1993).
45. S. P. Kampermann, T. M. Sabine, B. M. Craven, and R. K. McMullan, Hexamethylenetetramine: Extinction and thermal vibrations from neutron diffraction at six temperatures, *Acta Crystallogr.* **A51,** 489–497 (1995).
46. H. B. Bürgi, S. C. Capelli, and H. Birkedal, Anharmonicity in anisotropic displacement parameters, *Acta Crystallogr.* **A56,** 425–435 (2000).
47. I. Elvebredd and S. J. Cyvin, *in* "Molecular Structures and Vibrations" (S. J. Cyvin, Ed.), p. 283, Elsevier, Amsterdam (1972).
48. M. W. Thomas and R. E. Ghosh, Incoherent inelastic neutron scattering from hexamethylenetetramine and adamantane, *Mol. Phys.* **29,** 1489–1506 (1975).
49. J. E. Bertie and M. Solinas, Infrared and Raman spectra and the vibrational assignment of hexamethyletetramine-h12 and -d12, *J. Chem. Phys.* **61,** 1666–1677 (1974).
50. C. Ammann, P. Meier, and A. E. Merbach, A simple multinuclear NMR thermometer, *J. Magn. Reson.* **46,** 319–321 (1982).
51. D. Canet, G. C. Levy, and I. R. Peat, Time saving in ^{13}C spin-lattice relaxation measurements by inversion-recovery, *J. Magn. Reson.* **18,** 199–204 (1975).
52. J. Kowalewski, A. Ericsson, and R. Vestin, Determination of NOE factors using the dynamic Overhauser enhancement technique combined with a nonlinear least-squares fitting procedure, *J. Magn. Reson.* **31,** 165–169 (1978).
53. A. G. Palmer, N. J. Skelton, W. J. Chazin, P. E. Wright, and M. Rance, Suppression of the effects of cross-correlation between dipolar and anisotropic chemical shift relaxation mechanisms in the measurement of spin-spin relaxation rates, *Mol. Phys.* **75,** 699–711 (1992).
54. L. E. Kay, L. K. Nicholson, F. Delaglio, A. Bax, and D. A. Torchia, Pulse sequences for removal of the effects of cross correlation between dipolar and chemical-shift anisotropy relaxation mechanism on the measurement of heteronuclear T_1 and T_2 values in proteins, *J. Magn. Reson.* **97,** 359–375 (1992).
55. D. F. DeTar, *in* "Computer Programs for Chemistry," Vol. IV, p. 71, Academic Press, New York (1972).
56. D. Wallach and W. T. Huntress, Anisotropic molecular rotation in liquid N,N-dimethylformamide by NMR, *J. Chem. Phys.* **50,** 1219–1227 (1969).